Open-file Report 77-258

UNITED STATES
DEPARTMENT OF THE INTERIOR
GEOLOGICAL SURVEY

AEROMAGNETIC MAPS WITH GEOLOGIC INTERPRETATIONS FOR THE TULAROSA VALLEY, SOUTH-CENTRAL NEW MEXICO

By

G. D. Bath

CONTENTS

ILLUSTRATIONS

AEROMAGNETIC MAPS WITH GEOLOGIC INTERPRETATIONS FOR THE TULAROSA VALLEY, SOUTH-CENTRAL NEW MEXICO

By

G. D. Bath

ABSTRACT

An aeromagnetic survey of the Tularosa Valley in south-central New Mexico has provided information on the igneous rocks that are buried beneath alluvium and colluvium. The data, compiled as residual magnetic anomalies, are shown on twelve maps at a scale of 1:62,500. Measurements of magnetic properties of samples collected in the valley and adjacent highlands give a basis for identifying the anomaly-producing rocks. Precambrian rocks of the crystalline basement have weakly induced magnetizations and produce anomalies having low magnetic intensities and low magnetic gradients. Late Cretaceous and Cenozoic intrusive rocks have moderately to strongly induced magnetizations. Precambrian rocks produce prominent magnetic anomalies having higher amplitudes and higher gradients. The Quaternary basalt has a strong remanent magnetization of normal polarity and produces narrow anomalies having high magnetic gradients. Interpretations include an increase in elevation to the top of buried Precambrian rock in the northern part of the valley, a large Late Cretaceous and Cenozoic intrusive near Alamogordo, and a southern extension of the intrusive rock exposed in the Jarilla Mountains. Evidence for the southern extension comes from a quantitative analysis of the magnetic anomalies.

INTRODUCTION

This report releases to the open files twelve aeromagnetic maps and the geologic interpretations of these maps that were discussed by Bath, Healey, and Karably (1977) at the South-Central meeting of the Geological Society of America in El Paso, Texas. The maps were compiled by the U.S. Naval Oceanographic Office from a 1975 aeromagnetic survey for Project Magnet. The area is about 50 km wide and extends about 160 km northward from the New Mexico–Texas State line. Most of the area is within the boundaries of the White Sands Missile Range and the Fort Bliss Military Reservation. The survey and interpretations were undertaken for the Air Force Weapons Laboratory, Kirtland Air Force Base, New Mexico.

AEROMAGNETIC MAPS

Figures 1-12 are aeromagnetic maps showing the magnetic anomalies in total intensity that were measured August 2, 3, and 4, 1975, by Project Magnet of the U.S. Naval Oceanographic Office. The 1:62,500 scale was selected for the maps to permit comparison with features given on U.S. Geological Survey topographic maps. In addition, Fernald and Corchary (1976) have compiled a reconnaissance surficial geologic map of part of the valley at a scale of 1:125,000.

The aeromagnetic survey consisted of traverses flown about 10° west of north, about 2 km apart, and at about 1,737 m (5,700 ft) average barometric elevation. A magnetometer was set up at Kirtland Air Force Base to monitor daily variations in the Earth's magnetic field, and this information combined with data from the Tucson Magnetic Observatory was used to remove daily variations from the aeromagnetic data. Residual magnetic anomalies were determined by subtracting the 1975 Reference Field of the World Chart of the Earth's Magnetic Field from the aeromagnetic data.

Figures 13 and 14 were compiled at a scale of 1:400,000 to provide a regional representation of both the aeromagnetic anomalies and the buried rock structures that produce them. Figure 13 includes the data from figures 1-6 in the northern half of the valley, and figure 14 includes the data from figures 7-12 in the southern half of the valley. The capital letters shown on the figures are used to designate specific anomalous areas.

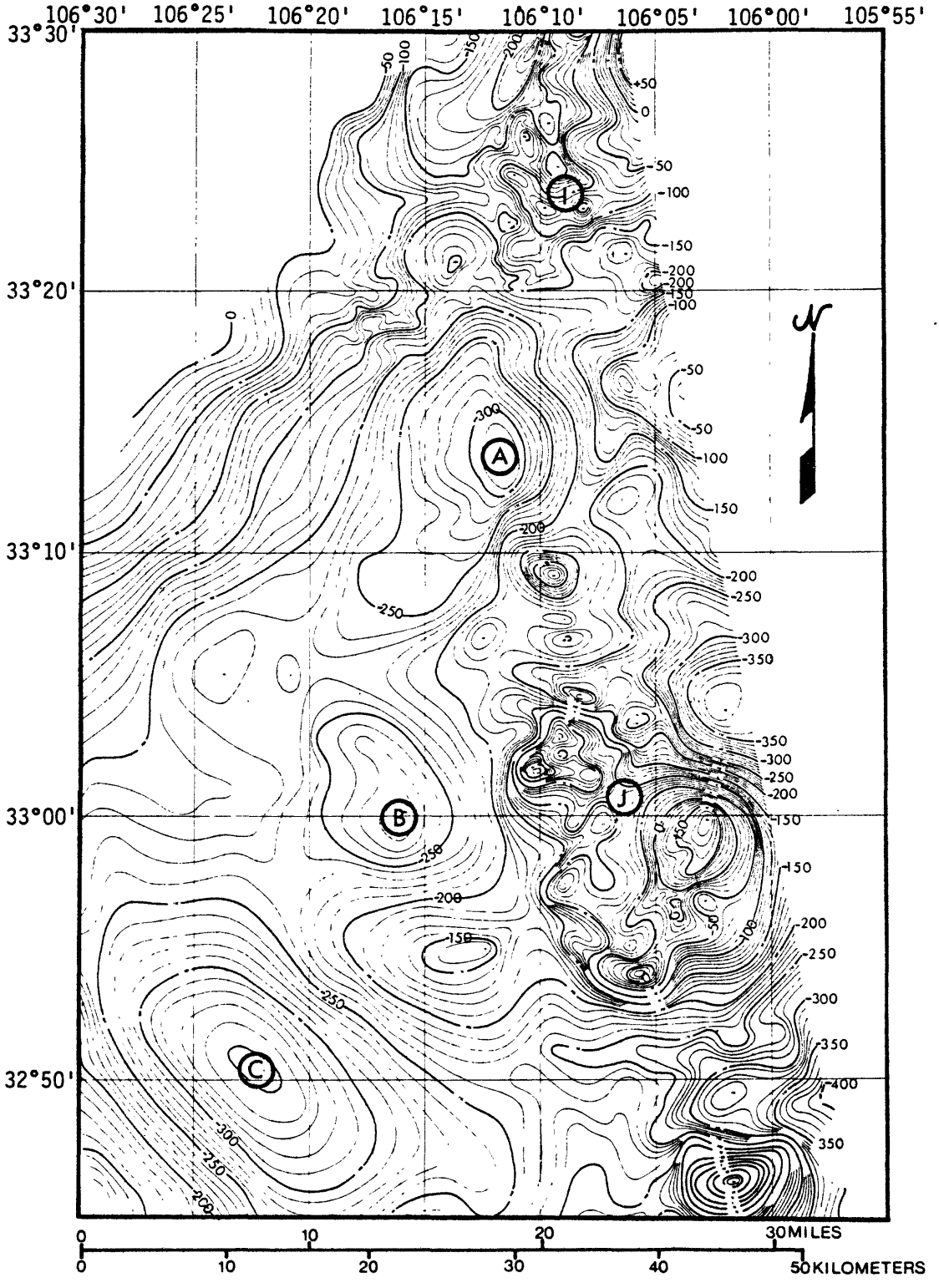

Figure 13.--Aeromagnetic map of the northern half of Tularosa Valley. The map was compiled at a scale of 1:400,000 from the data of figures 1-6. Letters designate anomalies described in the text.

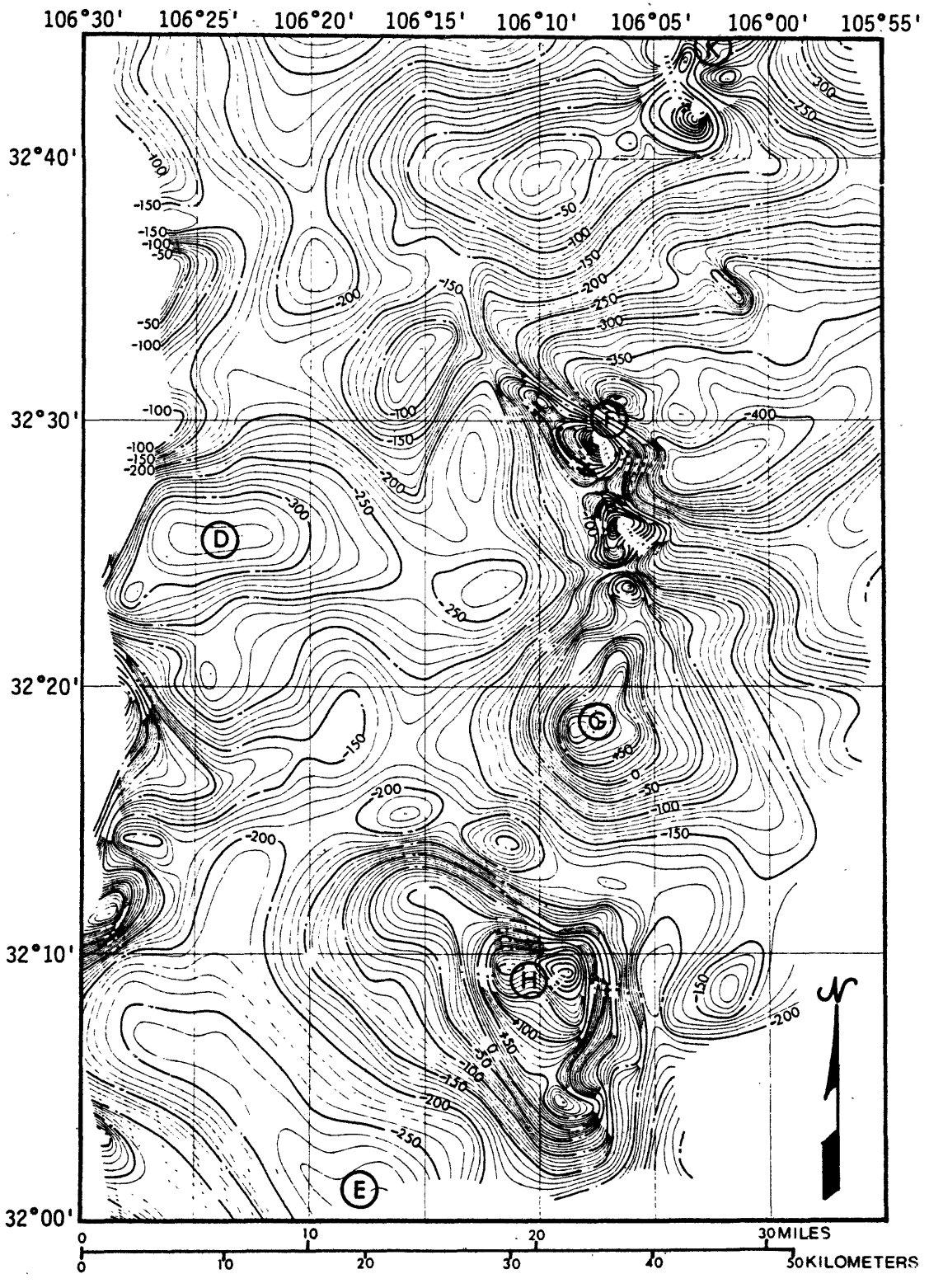

Figure 14.--Aeromagnetic map of the southern half of Tularosa Valley. The map was compiled at a scale of 1:400,000 from the data of figures 7-12. Letters designate anomalies described in the text.

MAGNETIC PROPERTIES AND GEOLOGIC SETTING

Magnetic properties of rock samples collected from outcrops in the valley and adjacent highlands were measured to give a basis for identification of the anomaly-producing rocks. The first step in the interpretation was an attempt to classify anomalies as arising from either Precambrian rock, Late Cretaceous and Cenozoic intrusive rocks, or Tertiary extrusive rocks. Figure 15 is an index map of Tularosa Valley that shows rock outcrops sampled and inferred positions of valley faults. The geologic data were taken from the 1:1,000,000 tectonic map of the Rio Grande region by Woodward and others (1975), which represents a compilation of detailed map data. Outcrops sampled included Precambrian intrusive and metamorphic rocks from east side of San Andres Mountains; Late Cretaceous and Cenozoic intrusive rocks from Jarilla and Organ Mountains and Salinas Peak; and Quaternary basalt field in the northernmost part of the valley. Magnetic properties for 90 roughhewn samples collected at 20 sites, which were measured using the method of Jahren and Bath (1967), are listed by Bath (1976, table 1).

The following "magnetic stratigraphy" is postulated from the values of magnetic properties along with considerations of the regional geology (Foster and Stipp, 1961; Dane and Bachman, 1965). Precambrian rocks of the crystalline basement have weak magnetizations and produce anomalies having low magnetic intensities and low magnetic gradients. Paleozoic sedimentary rocks are nonmagnetic. Late Cretaceous and Cenozoic intrusive rocks have moderate-to-strong magnetizations. Relative to Precambrian rocks, these produce prominent magnetic anomalies having higher amplitudes and higher gradients. Quaternary basalt, in the northern part of the valley, produces narrow anomalies having high magnetic gradients. All the intrusive rocks have induced magnetic intensities that are much greater than their remanent intensities, and the Koenigsberger's Q ratio is 0.2. The Quaternary basalt has remanent intensities that are much greater than their induced intensities, and the Q ratio is 30. None of the rock units sampled showed a reversed remanent polarity.

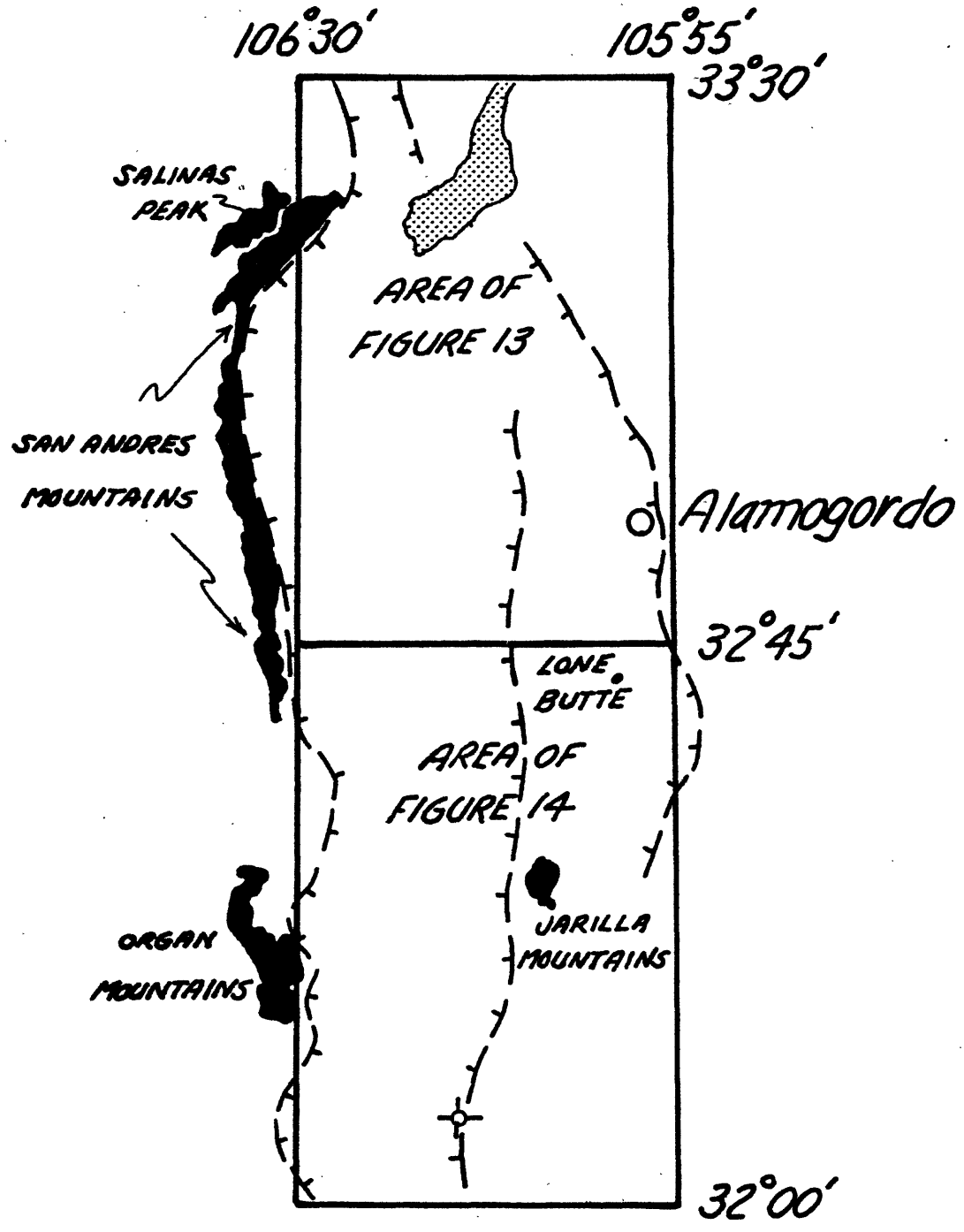

Figure 15.—Index map of Tularosa Valley showing areas of figures 13 and 14, mountainous areas where intrusive and metamorphic rocks were sampled (in black), area where extrusive rocks were sampled (stippled), and inferred valley faults. Hachures are on the downthrown side of normal faults. Geologic data are from Woodward and others (1975).

INTERPRETATION OF ANOMALIES

Only two of the prominent magnetic anomalies of figures 1-14 are positioned over topographic features that contain magnetized rock. The single anomaly having a maximum of 555 gammas, in the northeastern corner of figure 18, appears over Lone Butte shown in figure 15; and the complex anomaly having a maximum of 745 gammas, in the central part of figure 18, appears over the Jarilla Mountains shown in figure 15. All other prominent anomalies come from sources that are unknown and buried beneath nonmagnetic alluvium and colluvium.

The preponderance of anomalies having low magnetic gradients and intensities over the western part of the valley is consistent with an interpretation of deeply buried magnetic rocks. Low gradients and intensities are expected from magnetic rock at depth. To the east, gradients and intensities are higher, magnetic rocks are nearer the surface and the rocks are actually exposed in two places. Also, the normal fault of Woodward and others (1975) along the valley axis indicates that the valley structure consists of a low-standing side on the west and a high-standing side on the east. The normal fault is shown on figure 15.

Residual anomalies

The residual anomaly values determined by subtracting the International Geomagnetic Reference Field (IGRF) are too negative to be credible in areas of low magnetic gradient in the western part of figures 13 and 14. For example, the values at A, B, C, D, and E average about -300 gammas; and the average is too low to be explained by weakly magnetized Precambrian rock. A more likely possibility is the one proposed by Regan and Cain (1975), that removal of IGRF may result in anomalies having an unrealistic zero datum.

A better zero datum was obtained by using a surface-fitting method. The residual anomalies were sampled at 5-km intervals on a 5-km grid of the valley, and a least-squares adjustment of 321 samples provided the following equation for a planar surface:

$$T(x,y)=C_1x+C_2y+C_3. \quad (1)$$

$T(x,y)$ is the value, in gammas, computed for east coordinate x and north coordinate y; C_1 equals -0.58 gammas per kilometer, C_2 equals -0.01 gammas per kilometer, and C_3 equals -162.56 gammas at lat 32° N. and long 106°35' E. The planar surface was subtracted from the IGRF residual anomalies to prepare new residual anomalies and a new zero contour datum, as shown in figure 16 for the southernmost part of the valley. The zero datum was thereby increased by about 190 gammas.

In equation (1), the effects from constants C_1 and C_2 are small within the surveyed area. The constants were therefore omitted from the following equation that was used to compile the generalized anomalies of figures 17 and 18:

$$T(x,y)=C_3 \quad (2)$$

where C_3 equals -190 gammas.

Figures 17 and 18 show the data of figures 13 and 14 at a 100-gamma contour interval after the datum shift of +190 gammas. The figures give locations of maximum and minimum anomaly values; outcrops of Precambrian rock, Late Cretaceous and Cenozoic intrusives, and Quaternary basalt; capital letters identify specific anomalous areas.

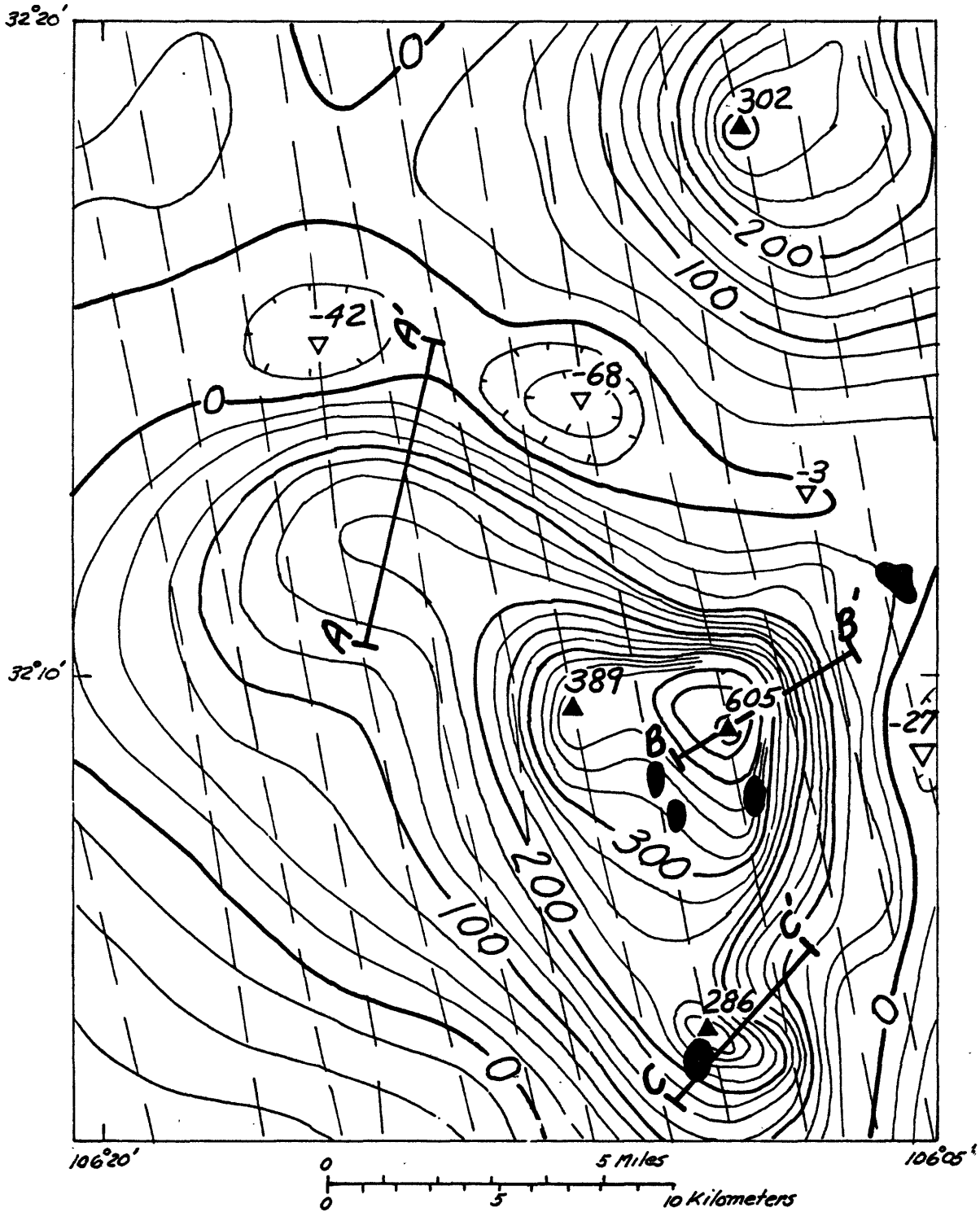

Figure 16.--Residual aeromagnetic map of southeastern part of Tularosa Valley showing 25-gamma contour interval from equation (1); paths of flight traverses flown 12° west of north along the valley; values of maxima, ▲, and minima, ▽, along flight traverses; shaded outlines show exposures of older sediments reported by Dane and Bachman (1965). Anomalies shown along profiles A-A', B-B', and C-C' are analyzed in figures 19, 20, and 21, respectively.

Northern area

The prominent anomalies of figure 17 include lows along the western and southwestern parts of the valley, a high to the northwest, and highs with associated bipolar lows along the eastern half of the valley. Bipolar lows are the negative anomalies that are offset to the north of bodies magnetized normally along the direction of the Earth's magnetic field.

Extensive areas of negative anomaly are attributed to an increase in thickness of nonmagnetic alluvium and older sediments that overlie magnetized Precambrian rock. Precambrian rock probably underlies the nonmagnetic sediments in the area of negative anomaly along the western half of the valley, and the minima at A, B, and C thus indicate areas of thicker sediments.

The prominent positive anomalies are attributed to a decrease in thickness of nonmagnetic sediments overlying either Precambrian rock or large masses of younger igneous rock. For example, in the northwestern corners of figures 13 and 17, the northward increase in magnetic intensity indicates an increase in elevation to the top of buried magnetized rock. The buried rock is designated Precambrian because of the low anomaly gradient and the nearby outcrops of Precambrian rocks along the San Andres Mountains. Intrusive rock at Salinas Peak is the only other nearby exposure of igneous rock, and magnetic property measurements revealed that it is nonmagnetic. An anomaly maximum would be expected in the vicinity of the Precambrian rock had the aeromagnetic survey been extended northward into this area.

An inferred thick mass of normally magnetized igneous rock is outlined by the 100-gamma contour at J. The bipolar low to the north reaches a minimum of -195 gammas. The mass is probably a Late Cretaceous and Cenozoic intrusive, but a thick accumulation of volcanic rock or a Precambrian intrusive having higher than average magnetization also are possible explanations. The +145-gamma anomaly in the southeast corner of figure 17 is probably caused by a Late Cretaceous and Cenozoic intrusive because of its close resemblance to the anomaly over nearby Lone Butte (fig. 18).

An irregular anomaly pattern was found over the Quaternary basalt field. The only prominent anomaly is at I, east of the basalt. Although the basalt is strongly magnetized, its thickness is only 20 m --presumably too thin to produce a prominent anomaly at the elevation datum of the aeromagnetic survey.

Southern area

A larger number of anomalies are shown in figures 14 and 18 for the southern part of Tularosa Valley, and several of the anomalies are positioned near or over outcrops of magnetic rock. Broad areas of negative anomaly, and the minima at D and E, indicate thick sections of nonmagnetic sediments overlying magnetic Precambrian rock along the western half of the valley. The positive anomalies are more narrow and they indicate a thinning of sediments (1) toward the western border of the aeromagnetic survey near outcrops of Precambrian rock and the outcrop of Late Cretaceous and Cenozoic intrusive in the Organ Mountains; (2) near exposures of Late Cretaceous and Cenozoic intrusives in the areas of Lone Butte at K and Jarilla Mountains at F; and (3) over buried magnetic rock of unknown identity at G and H.

No distinctive anomalies were found at some outcrops of igneous rock. The absence of anomalies over basalt north of Jarilla Mountains and south of Organ Mountains indicates the basalt is thin or weakly magnetic. The absence of anomalies near intrusive exposures north of Jarilla Mountains and in the southeastern corner of figure 18 indicates the Late Cretaceous and Cenozoic intrusives have a nonmagnetic as well as a magnetic facies.

The positive anomalies at G and H appear to be the buried southern extension of the intrusive rocks at Jarilla Mountains. To test this possibility, the magnetic anomalies near H along lines A-A', B-B' and C-C' of figure 16 were analyzed using the method of Koulomzine, Lamontagne and Nadeau (1970) to gain information about geologic structure and magnetization of the anomaly-producing rocks. The method assumes that most of the source rocks are confined within a tabular, dikelike structure extending a large distance along its strike and dip directions. As shown in figures 19-21, conjugate points are selected to represent the anomaly, and these points are used to decompose the anomaly into symmetrical and antisymmetrical components. The components are then analyzed to obtain parameters that include center point (X_o), depth (h), width (w), and angle (Θ), for the anomaly-producing body. Hutchison (1958) and other geophysicists use Θ to classify a dikelike body as being either a dike or a sheet. The angle is defined by

$$\Theta = \tan^{-1} \frac{w}{2h} . \qquad (3)$$

Results indicate the broad positive anomaly near H in figure 18 can be explained by dikelike bodies that are less than 2 km wide, and are thus similar to the narrow bodies partly exposed at Jarilla Mountains. Also, the bodies have Θ angles that are less than 40°, and this permits application of the thin dike, or sheet, analysis of Gay (1963) to determine magnetization. Magnetizations are similar to those found at the Jarilla Mountains. The bodies are magnetized normally along the direction of the Earth's magnetic field, and their intensities are too high to be explained by our measurements of magnetic properties of Precambrian rock samples. Therefore, we conclude that anomalies G and H represent the southern extension of intrusive rock exposed in the Jarilla Mountains.

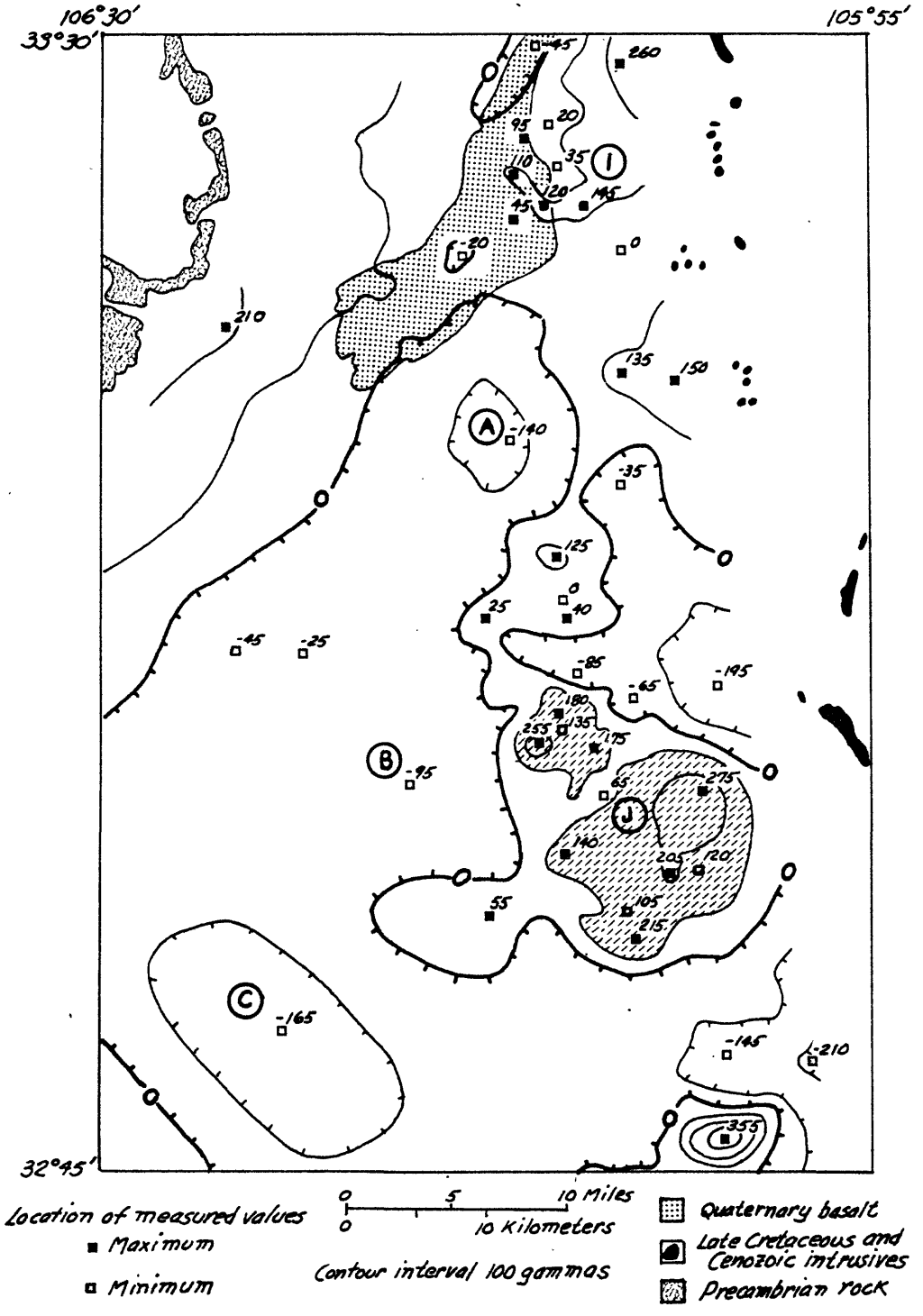

Figure 17.--Residual aeromagnetic and geologic interpretive map of northern part of Tularosa Valley. Zero and negative contours are hachured. Letters designate anomalies described in the text. The dashed diagonal lines outline inferred position of buried intrusives.

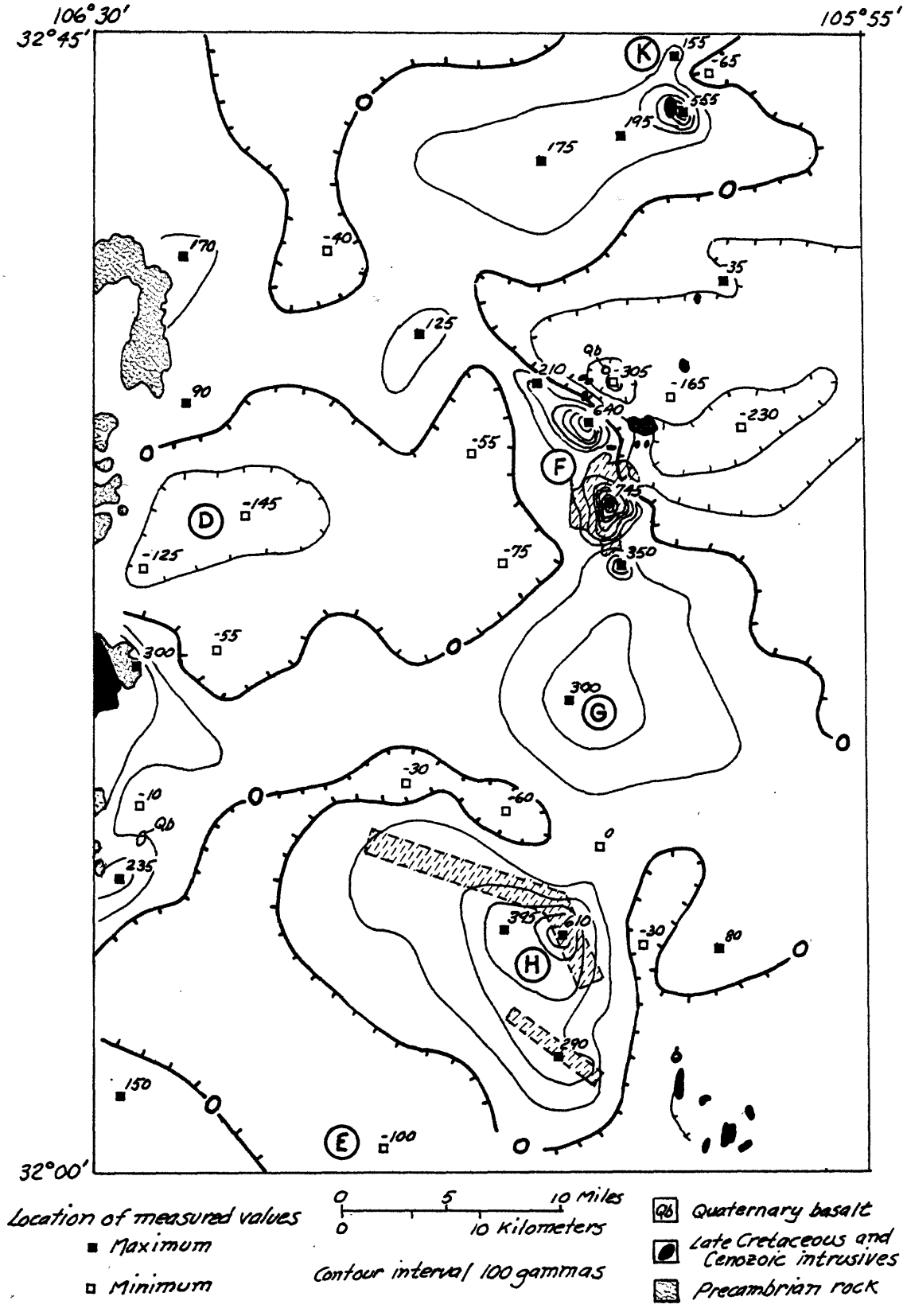

Figure 18.--Residual aeromagnetic and geologic interpretive map of southern part of Tularosa Valley. Zero and negative contours are hachured. Letters designate anomalies described in the text. The dashed diagonal lines outline the intrusive rock outcrops at Jarilla Mountains and the inferred positions of buried intrusives near H.

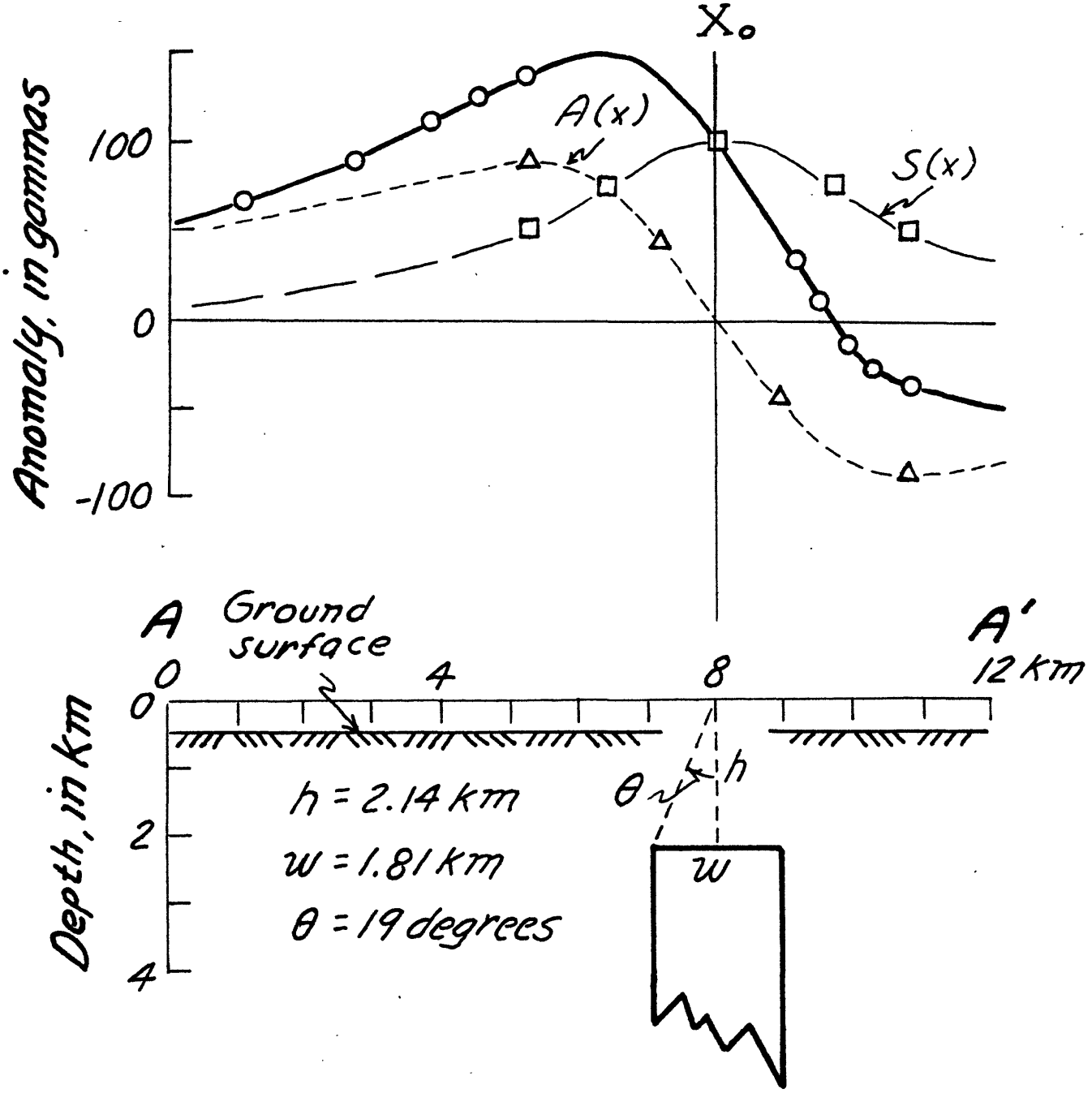

Figure 19.--Analysis of magnetic anomaly along profile A-A' of figure 16 to determine center point (X_o), depth (h), width (w), and angle θ, for anomaly-producing body. The solid line is the anomaly along A-A', and the circles are the conjugate points used to decompose the anomaly into symmetrical, S(x), and antisymmetrical, A(x), components. These components are then analyzed separately using the points indicated by squares and triangles. Zero depth is at elevation of aeromagnetic survey, and not at elevation of the ground surface.

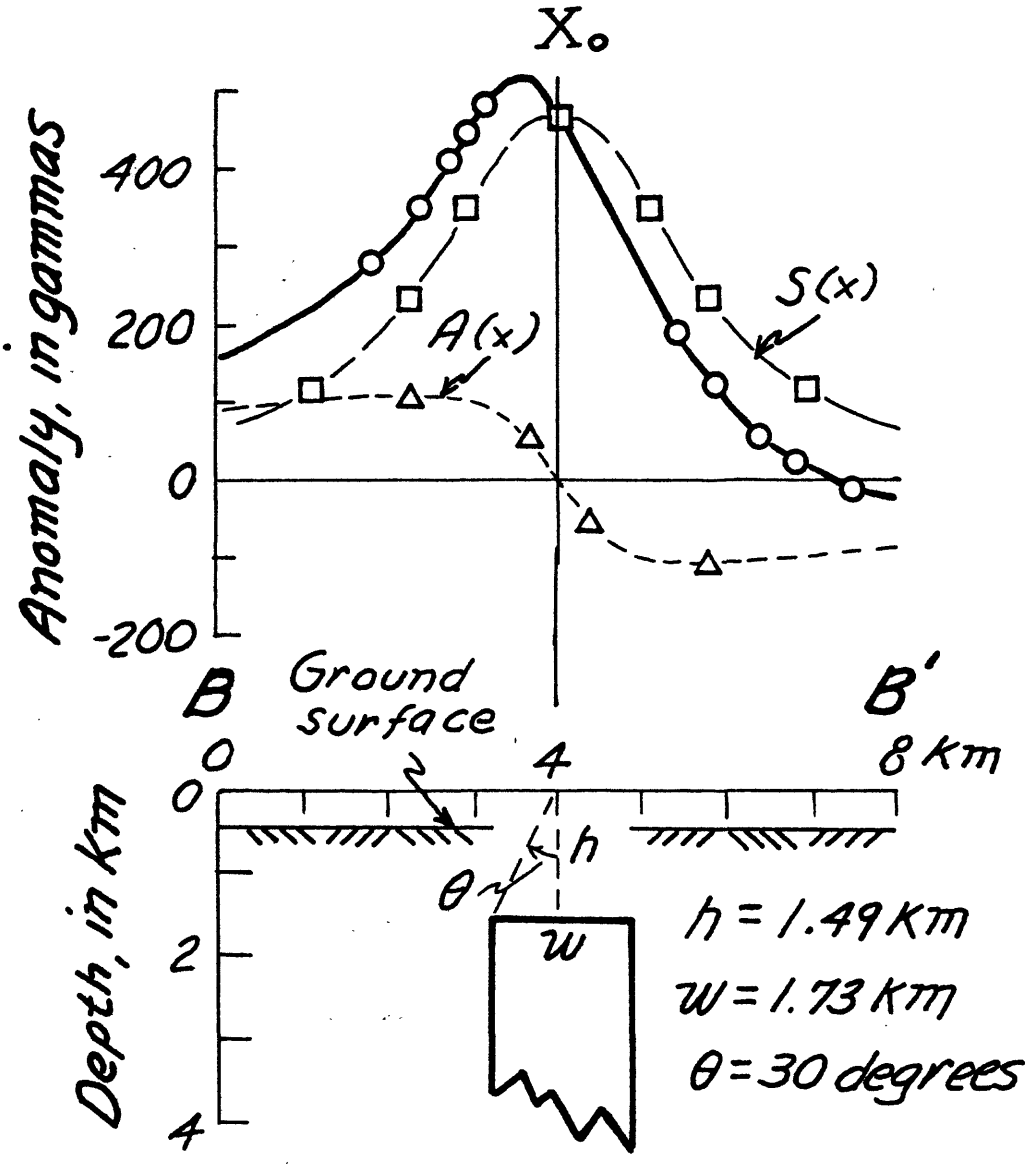

Figure 20.--Analysis of magnetic anomaly along profile B-B' of figure 16 to determine center point (X_o), depth (h), width (w), and angle θ, for anomaly-producing body. The solid line is the anomaly along B-B', and the circles are the conjugate points used to decompose the anomaly into symmetrical, S(x), and antisymmetrical, A(x), components. These components are then analyzed separately using the points indicated by squares and triangles. Zero depth is at elevation of aeromagnetic survey, and not at elevation at the ground surface.

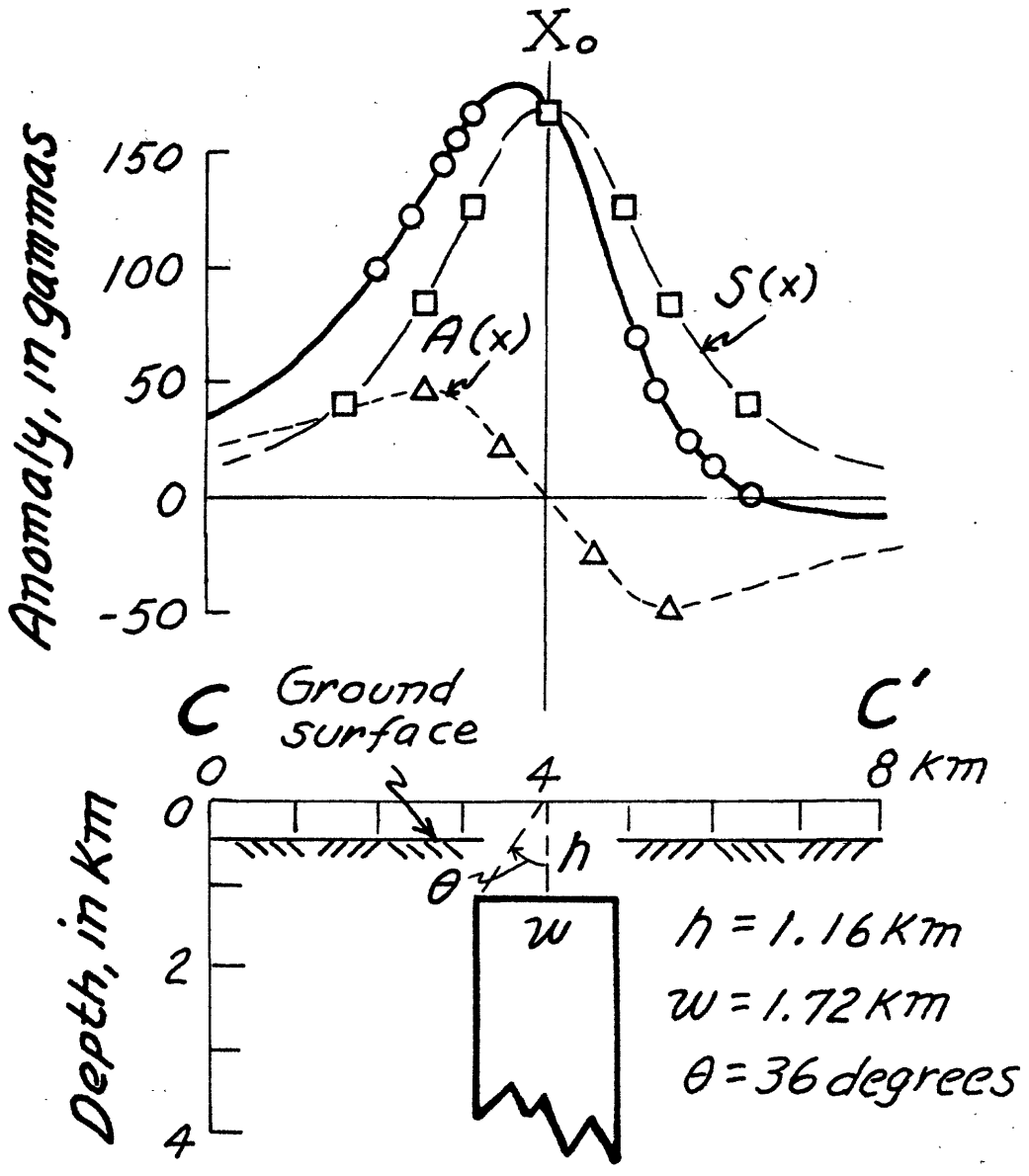

Figure 21.--Analysis of magnetic anomaly along profile C-C' of figure 16 to determine center point (X_o), depth (h), width (w), and angle Θ, for anomaly-producing body. The solid line is the anomaly along C-C', and the circles are the conjugate points used to decompose the anomaly into symmetrical, S(x), and antisymmetrical, A(x), components. These components are then analyzed separately using the points indicated by squares and triangles. Zero depth is at elevation of aeromagnetic survey, and not at elevation of the ground surface.

REFERENCES CITED

Bath, G. D., 1976, Interpretation of magnetic surveys in intermontane valleys of Nevada and southern New Mexico: U.S. Geol. Survey Open-file Report 76-440, 37 p.

Bath, G. D., Healey, D. L., and Karably, L. S., 1977, Combined analysis of gravity and magnetic anomalies at Tularosa Valley, New Mexico [abs.]: Geol. Soc. America, Abs. with Programs, v. 9, no. 1, p. 3-4.

Dane, C. H., and Bachman, G. O., 1965, Geologic map of New Mexico: Washington, D. C., U.S. Geological Survey, 2 sheets, scale 1:500,000.

Fernald, A. T., and Corchary, G. S., 1976, Map of northern portion of White Sands Missile Range, New Mexico, showing surface geology, in Neal, J. T. and others, Site investigation methodology for multiple aim point missile systems: Air Force Weapons Lab. AFWL-TR-76-145, p. 42; available from Kirtland Air Force Base.

Foster, R. W., and Stipp, T. F., 1961, Preliminary geologic and relief map of the Precambrian rocks of New Mexico: New Mexico Bur. Mines and Mineral Resources Circ. 57, 37 p.

Gay, P. S., 1963, Standard curves for interpretation of magnetic anomalies over long tabular bodies: Geophysics, v. 28, p. 161-200.

Hutchison, R., 1958, Magnetic analysis by logarithmic curves: Geophysics, v. 23, p. 749-769.

Jahren, C. E., and Bath, G. D., 1967, Rapid estimation of induced and remanent magnetization of rock samples, Nevada Test Site: U.S. Geol. Survey Open-file Report, 29 p.

Koulomzine, T., Lamontagne, Y., and Nadeau, A., 1970, New methods for the direct interpretation of magnetic anomalies caused by inclined dikes of infinite length: Geophysics, v. 35, p. 812-830.

Regan, R. D., and Cain, J. C., 1975, The use of geomagnetic field models in magnetic surveys: Geophysics, v. 40, p. 621-629.

Woodward, L. A., Callender, J. F., Gries, J., Seager, W. R., Chapin, C. E., Zilinski, R. E., and Shaffer, W. L., 1975, Tectonic map of the Rio Grande region: New Mexico Geol. Soc. Guidebook of the Las Cruces Country, 26th Ann. Field Conf., 1975, Las Cruces, New Mexico.

GPO 841-410